

Modulation structure in $\text{Bi}_2\text{Sr}_{1.8}\text{La}_{0.2}\text{Cu}_{1-x}\text{M}_x\text{O}_y$ ($M=\text{Fe, Co, Ni, and Zn}$)

Mao Zhiqiang, Zuo Jian, Tian Mingliang, Xu Gaojie, Xu Cunyi, Wang Yu, and Zhu Jingsheng
Structure Research Laboratory, University of Science and Technology of China, Hefei, Anhui, 230026, People's Republic of China

Zhang Yuheng

*Chinese Center of Advanced Science and Technology (World Laboratory), P.O. Box 8730, Beijing, People's Republic of China
 and Structure Research Laboratory, University of Science and Technology of China,
 Hefei, Anhui, 230026, People's Republic of China*

(Received 24 July 1995)

Transition-metal-doped $\text{Bi}_2\text{Sr}_{1.8}\text{La}_{0.2}\text{Cu}_{1-x}\text{M}_x\text{O}_y$ ($M=\text{Fe, Co, Ni, and Zn}$) samples were synthesized. X-ray diffraction analysis showed that these 3d elements had different solubility in $\text{Bi}_2\text{Sr}_{1.8}\text{La}_{0.2}\text{CuO}_y$. The limits of solid solution formation were at $x=0.5$ for the Fe system, $x=1.0$ for the Co system, and $x=0.1$ for the Ni and Zn systems. The effect of these 3d metal substitutions for Cu on the incommensurate modulation structure in $\text{Bi}_2\text{Sr}_{1.8}\text{La}_{0.2}\text{CuO}_y$ was examined by means of electron diffraction. The experimental results showed that all the substitutions of Fe, Co, Ni, and Zn for Cu decreased the modulation periodicity. It decreased from $4.32b$ at $x=0$ to $3.95b$ at $x=0.5$ for the Fe system, $3.82b$ at $x=1.0$ for the Co system, $4.24b$ at $x=0.1$ for the Ni system, and $4.18b$ at $x=0.1$ for the Zn system, respectively. In addition, the structure distortion characteristic related to the change in the incommensurate modulation was examined with Raman scattering. The experimental data showed that the vibration properties of the oxygen atoms in both Bi-O and Sr-O bondings also changed with the decrease in the modulation periodicity. This behavior can be considered a consequence of structural relaxation caused by the enhancement of the degree of crystal misfit.

I. INTRODUCTION

It is known that the structure of a series of Bi-based superconductors $\text{Bi}_2\text{Sr}_2\text{Ca}_{n-1}\text{Cu}_n\text{O}_{2n+4+\delta}$, $n=1, 2$, and 3 ($n=1, 2201$; $n=2, 2212$; $n=3, 2223$), can be described as an alternate stacking of Bi_2O_2 layers and Cu-containing perovskite components along the c direction.¹ The double BiO layers do not consist of perfect two-dimensional sheets, but contain an alternative distribution of Bi-concentrated bands and Bi-deficient bands. This type of arrangement of Bi atoms forms the superstructural modulation. The superlattice has orthorhombic symmetry in the 2212 and 2223 phases, but monoclinic in the 2201 phase. In order to clarify the origin of the superstructural modulation, numerous investigations have been made and several models have been proposed, mainly including (1) the extra-oxygen model,^{2,3} (2) crystal misfit model,^{4,5} (3) ordering of Sr vacancies,⁶ (4) regular substitution of Bi by (Ca, Sr) or Cu,⁷ and (5) changes in the orientation of Bi lone pairs.² Among these models the extra oxygen model has been most widely accepted. It indicates that the periodic intercalation of extra oxygen atoms in the Bi_2O_2 layers is responsible for the modulation and the extra oxygen is brought by the partial substitution of Bi^{5+} instead of Bi^{3+} . The model is basically successful in explaining the variations of modulation periodicity caused by the substitution with different valence cations,⁸ but failed in explaining the change of modulation caused by the substitution with same valence cations.⁹ In addition, Pham and co-workers reported that samples with different oxygen contents had modulated structures with the same modulation periodicity.¹⁰ They suggested that the presence of extra oxygen in the Bi_2O_2 layers could only be regarded as a consequence of the

particular geometry introduced by bismuth, but not as the origin of modulation.

In our previous work, we found the crystal misfit model much more successful in interpreting the modulation-vector change induced by doping with either different or the same valence elements.^{9,11} The earliest crystal misfit model was put forth by Gai, Subramanian, and Sleight.⁴ This model indicates that the superstructural modulation of Bi cuprates comes from the crystal misfit along the b axis between the Bi_2O_2 layers and perovskite blocks. The presence of extra oxygen atoms in the Bi_2O_2 layers can be regarded as a consequence caused by the crystal misfit. In the Gronoble conference in 1994, Amelinckx and Van Tendeloo also pointed out that the fundamental reason for the modulation seems to be lattice misfit between the perovskite block and the bismuth oxide layers.¹² To further examine the validity of the crystal misfit model, we studied the modulation structure of the transition-metal- (Fe, Co, Ni, and Zn) doped $\text{Bi}_2\text{Sr}_{1.8}\text{La}_{0.2}\text{CuO}_y$ series. The addition of La in the $\text{Bi}_2\text{Sr}_{1.8}\text{La}_{0.2}\text{Cu}_{1-x}\text{M}_x\text{O}_y$ series was to suppress the presence of the second phase.⁹ Our experiment results showed that all the substitutions of Fe, Co, Ni, and Zn for Cu reduced the modulation periodicity. For the Fe- and Co-doped systems, Yanagisawa and co-workers have attempted to use the extra oxygen model to explain the observed variations of the modulation.¹³ However, our Raman scattering investigation on the $\text{Bi}_2\text{Sr}_{1.8}\text{La}_{0.2}\text{Cu}_{1-x}\text{M}_x\text{O}_y$ ($M=\text{Fe, Co, Ni, and Zn}$) series showed that it was inappropriate to use the extra oxygen model to explain the change in the modulation structure caused by the Fe and Co dopings. But the crystal misfit model gives a better interpretation.

TABLE I. Structure parameters of $\text{Bi}_2\text{Sr}_{1.8}\text{La}_{0.2}\text{Cu}_{1-x}\text{Co}_x\text{O}_y$. The error in the lattice parameters is about 2/1000.

Co content x	a (Å)	b (Å)	c (Å)	q_b/b
0	5.376	5.372	24.536	4.32
0.2	5.395	5.378	24.196	4.28
0.4	5.414	5.399	24.015	4.25
0.6	5.416	5.403	23.695	4.18
0.8	5.436	5.425	23.383	4.02
1.0	5.458	5.435	23.306	3.82

II. EXPERIMENTAL METHODS

Samples of $\text{Bi}_2\text{Sr}_{1.8}\text{La}_{0.2}\text{Cu}_{1-x}\text{M}_x\text{O}_y$ ($M = \text{Fe}, \text{Co}, \text{Ni}$, and Zn) were prepared by a conventional solid-state reaction method using high-purity powders of Bi_2O_3 , SrCO_3 , La_2O_3 , Fe_2O_3 , Co_2O_3 , NiO , ZnO , and CuO . First, the appropriate mixture of these powders was well ground and preheated at 810–850 °C in air for 36 h with an intermediate grinding. The loose powder was reground and pressed into dish-shaped pellets. The pellets were sintered in the temperature range of 885–930 °C in flowing oxygen. The repeated grindings and sinterings were necessary to ensure uniform distribution of dopants. Finally, the samples were quenched in air.

An x-ray diffraction (XRD) analysis was carried out with a Rigaku-D/max- γ A diffractometer using monochromatic high-intensity Cu $K\alpha$ radiation at room temperature. Electron diffraction (ED) patterns were obtained using an H-800 transmission electron microscope (TEM), and the specimens for TEM observations were prepared by the crushing method. Raman spectra were measured on a Spex-1403 Raman spectrophotometer using a backscattering technique. The 5145-Å line from an argon-ion laser was used as an excitation light source. All measurements were made at room temperature, and each spectrum shown was taken with refocusing on at least two different spots to assure reproducibility.

III. EXPERIMENTAL RESULTS

A. XRD analysis of the $\text{Bi}_2\text{Sr}_{1.8}\text{La}_{0.2}\text{Cu}_{1-x}\text{M}_x\text{O}_y$ ($M = \text{Fe}, \text{Co}, \text{Ni}$, and Zn) samples

To screen for the second phases or structure changes, a powder XRD analysis was carried out for each doped sample. The experimental data showed that the 3d elements Fe, Co, Ni, and Zn were all soluble in $\text{Bi}_2\text{Sr}_{1.8}\text{La}_{0.2}\text{Cu}_{1-x}\text{M}_x\text{O}_y$. But the solid solubility differed with each type of doping. The limits of solid solution formation were at $x = 0.5$ with the Fe-doped system, $x = 1.0$ with the Co-doped system, and $x = 0.1$ with both the Ni- and Zn-doped systems. From XRD data, the lattice parameters for each doped sample were calculated using a least-squares refinement. Tables I–IV give the obtained results. For the Fe- and Co-doped series, Tables I and II show that the lattice parameters a and b increase with increasing x , while the parameter c decreases accordingly. This type of change in the lattice parameters with doping concentration in the Fe and Co systems was slightly different from the results reported by Tarascon *et al.*,¹⁴ which might be due to the difference in the sample preparing conditions. For the Ni- and

TABLE II. Structure parameters of $\text{Bi}_2\text{Sr}_{1.8}\text{La}_{0.2}\text{Cu}_{1-x}\text{Fe}_x\text{O}_y$.

Fe content x	a (Å)	b (Å)	c (Å)	q_b/b
0.2	5.385	5.376	24.170	4.20
0.3	5.396	5.384	23.917	4.12
0.4	5.416	5.395	23.828	4.09
0.5	5.432	5.413	23.704	3.95

Zn-doped systems, the results shown in Tables III and IV show that both Ni and Zn substitutions also increase the lattice parameters a and b and reduce the lattice parameter c .

B. ED analysis of the $\text{Bi}_2\text{Sr}_{1.8}\text{La}_{0.2}\text{Cu}_{1-x}\text{M}_x\text{O}_y$ ($M = \text{Fe}, \text{Co}, \text{Ni}$, and Zn) samples

To determine the evolution of the superstructural modulation upon increasing the doping content within the $\text{Bi}_2\text{Sr}_{1.8}\text{La}_{0.2}\text{Cu}_{1-x}\text{M}_x\text{O}_y$ series, we measured the modulation periodicity along the b direction, q_b , for the samples with different doping levels using the ED pattern along [001]-zone axis. The obtained results are also listed in Tables I–IV. All the substitutions of Fe, Co, Ni, and Zn reduced the modulation periodicity within the limits of solid solution. The modulation periodicity decreased from $4.32b$ at $x = 0$ to $3.95b$ at $x = 0.5$ for the Fe system, $3.82b$ at $x = 1.0$ for the Co system, $4.24b$ at $x = 0.1$ for the Ni system, and $4.18b$ at $x = 0.1$ for the Zn system. Though Fe, Co, Ni, and Zn dopings reduced the modulation periodicity of the Bi-2201 phase, they did not change the symmetry of the superlattice. Figure 1 displays the most representative ED patterns of the Fe and Co systems. It shows that the modulation still remains monoclinic incommensurate at the limit of the solid solution. For the Fe and Co systems, a previous study made by Yanagisawa *et al.*¹³ revealed that the superstructure modulation not only reduced in periodicity upon increasing the doping content, but also transitioned from monoclinic incommensurate to orthorhombic commensurate near the limits of the solid solution. It is obvious that the difference between our results and the reported ones comes from the difference in the modulation characteristic of the undoped parent compound.

Figure 2 shows the dependence of the modulation periodicity (q_b) on the lattice parameter b for the $\text{Bi}_2\text{Sr}_{1.8}\text{La}_{0.2}\text{Cu}_{1-x}\text{M}_x\text{O}_y$ ($M = \text{Fe}, \text{Co}, \text{Ni}$, and Zn) series. In the four doped systems, a decrease in q_b exhibits a different manner with an increase of the parameter b . The decrease in the modulation periodicity caused by the Fe doping is the most pronounced among the four doped systems.

TABLE III. Structure parameters of $\text{Bi}_2\text{Sr}_{1.8}\text{La}_{0.2}\text{Cu}_{1-x}\text{Ni}_x\text{O}_y$.

Ni content x	a (Å)	b (Å)	c (Å)	q_b/b
0.02	5.379	5.373	24.530	
0.04	5.382	5.375	24.522	
0.06	5.384	5.378	24.485	4.28
0.08	5.387	5.380	24.403	
0.10	5.396	5.390	24.389	4.24

TABLE IV. Structure parameters of $\text{Bi}_2\text{Sr}_{1.8}\text{La}_{0.2}\text{Cu}_{1-x}\text{Zn}_x\text{O}_y$.

Zn content x	a (Å)	b (Å)	c (Å)	q_b/b
0.02	5.378	5.373	24.515	
0.04	5.384	5.376	24.493	
0.06	5.386	5.377	24.394	4.24
0.08	5.389	5.379	24.380	
0.10	5.399	5.389	24.334	4.18

C. Raman scattering analysis of the $\text{Bi}_2\text{Sr}_{1.8}\text{La}_{0.2}\text{Cu}_{1-x}\text{M}_x\text{O}_y$ ($M=\text{Fe}, \text{Co}, \text{Ni},$ and Zn) samples

In order to examine the structure distortion associated with the change in the superstructural modulation, Raman scattering analyses were carried out for each group of doped samples. Figures 3(b) and 3(c) show the Raman spectra of the $\text{Bi}_2\text{Sr}_{1.8}\text{La}_{0.2}\text{Cu}_{1-x}\text{M}_x\text{O}_y$ ($M=\text{Fe}, x=0.1, 0.2, 0.3, 0.4,$ and 0.5 ; $M=\text{Co}, x=0.2, 0.4, 0.6,$ and 0.8) samples in the frequency range of $215\text{--}800\text{ cm}^{-1}$. For the samples with lower dopant concentration, two stronger Raman modes at ~ 450 and 615 cm^{-1} were clearly observed within this frequency range. In the light of the assignment of the phonon Raman modes of the Bi-2201 phase in Refs. 15 and 16, the phonon modes observed in the Raman spectra of the $\text{Bi}_2\text{Sr}_{1.8}\text{La}_{0.2}\text{Cu}_{1-x}\text{M}_x\text{O}_y$ ($M=\text{Fe}$ and Co) samples could be assigned. That is, the 450- and 615-cm^{-1} lines corresponded, respectively, to the A_g mode of vibration of O_{Sr} atoms along the c axis and to the A_g mode of vibration of O_{Bi} atoms along the a axis (O_{Sr} and O_{Bi} refer to the oxygen atoms in the SrO and Bi_2O_2 layers, respectively). For the samples with higher doping levels ($x>0.2$), the $\sim 450\text{-}$ and 615-cm^{-1} lines reduced in intensity and increased in linewidth obviously with increasing dopant concentration in both Fe- and Co-doped systems. At the same time, the 615-cm^{-1} line shifted toward the lower-frequency side. There is no doubt that this type of change in the Raman mode came from the structural distortion connected with the change in the modulation structure. A detailed discussion is given below. From the comparison of the Raman spectra of the Fe and Co systems, we found that broadening in the Raman spectra caused by the Fe doping was more serious than that caused by the Co doping at the same dopant concentration. In addition, another noteworthy point for the Raman spectra (shown in Fig. 3) was that the line shape of the Raman peak of $\sim 615\text{ cm}^{-1}$ was asymmetric and a weaker broadening at the higher frequency side of this line was observed for each doped sample. In

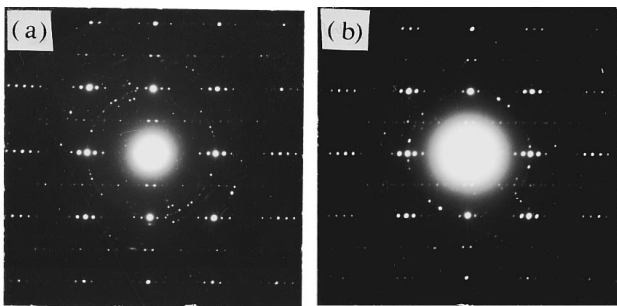


FIG. 1. (a) [001] ED pattern of the $\text{Bi}_2\text{Sr}_{1.8}\text{La}_{0.2}\text{Cu}_{0.5}\text{Fe}_{0.5}\text{O}_y$ sample, (b) [001] ED pattern of the $\text{Bi}_2\text{Sr}_{1.8}\text{La}_{0.2}\text{CoO}_y$ sample.

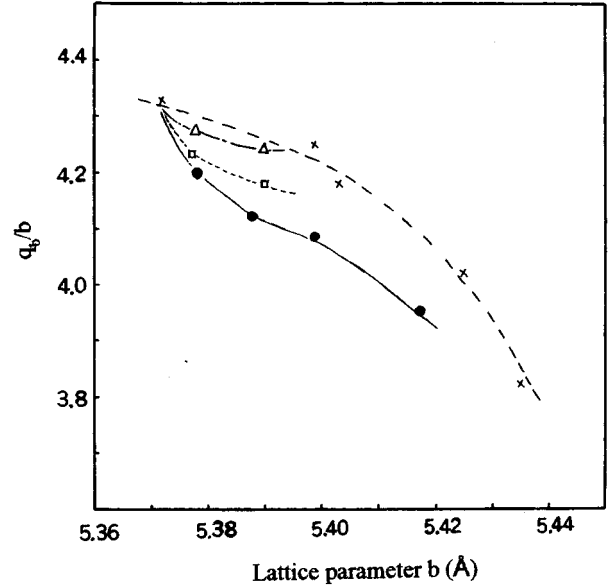


FIG. 2. Dependence of the modulation periodicity, q_b , on the lattice parameter b in the $\text{Bi}_2\text{Sr}_{1.8}\text{La}_{0.2}\text{Cu}_{1-x}\text{M}_x\text{O}_y$ ($M=\text{Fe}, \text{Co}, \text{Ni},$ and Zn) series; \bullet $M=\text{Fe}$; \square $M=\text{Zn}$; \triangle $M=\text{Ni}$; \times $M=\text{Co}$.

general, in the undoped $\text{Bi}_2\text{Sr}_2\text{CuO}_y$ system, a weak shoulder peak around 660 cm^{-1} appeared at the higher-frequency side of the 630-cm^{-1} mode. Cardona and co-workers ascribed the presence of such a shoulder peak to the vibration of the extra oxygen atoms of the Bi_2O_2 layers.¹⁵ In Fe- and Co-doped samples, though no obvious shoulder peak at the higher-frequency side of the 615-cm^{-1} line was detected, the broadening of Raman mode around 645 cm^{-1} could also be considered to be from the vibration of the extra oxygen atoms in the Bi_2O_2 layers.

Figures 4(a) and 4(b) show the Raman spectra of the $\text{Bi}_2\text{Sr}_{1.8}\text{La}_{0.2}\text{Cu}_{1-x}\text{M}_x\text{O}_y$ ($M=\text{Ni}$ and Zn) samples. A remarkable difference between the Raman spectra of the two doped systems was observed. The vibration mode of the O_{Sr} atoms only exhibited a slight broadening in the Ni-doped sample, while in the Zn-doped system the O_{Sr} phonon mode broadened severely upon increasing Zn content. However, the vibration mode of the O_{Bi} atoms located at $\sim 630\text{ cm}^{-1}$ did not show obvious change with Ni and Zn dopings. In the Raman spectra of the Ni- and Zn-doped systems, a weaker line with the frequency of 315 cm^{-1} was simultaneously observed besides the 460- and 630-cm^{-1} modes. This line was generally assigned to the vibration mode of the O_{Sr} atoms along the a axis.¹⁷ This 315-cm^{-1} line basically remained unchanged with increasing Ni content, but weakened more and more with increasing Zn content. This suggests that the Zn doping has a stronger influence on the vibration characteristic of the apical oxygen atoms in the SrO layers than the Ni doping.

IV. DISCUSSION

A. Explanation for the change in the modulation structure caused by Fe, Co, Ni, and Zn substitutions for Cu

For the $\text{Bi}_{2.1}\text{Sr}_{1.9-x}\text{La}_x\text{CuO}_y$ system, our previous work indicates that the La^{3+} substitution for Sr^{2+} decreases the

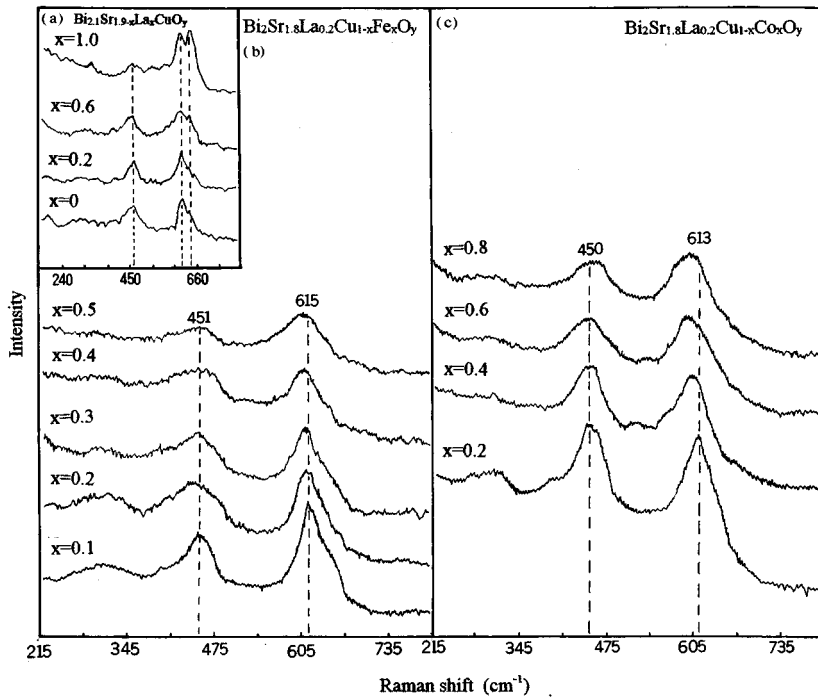


FIG. 3. Raman spectra in $\text{Bi}_2\text{Sr}_{1.8}\text{La}_{0.2}\text{Cu}_{1-x}\text{M}_x\text{O}_y$ ($M=\text{Fe}$ and Co); the inset shows the Raman spectra in $\text{Bi}_{2.1}\text{Sr}_{1.9-x}\text{La}_x\text{CuO}_y$ (taken from Ref. 16).

modulation periodicity.⁹ Raman scattering analysis¹⁸ shows that the vibration mode of the extra oxygen atoms in the Bi_2O_2 layers intensifies strikingly with increasing La content and two peaks at 613 and 646 cm^{-1} can be resolved clearly with $x=1.0$, as shown in the inset of Fig. 3. This suggests that the Bi_2O_2 layers accept the extra oxygen introduced by the La^{3+} substitution for Sr^{2+} and that the decrease in the modulation periodicity might be related to the increase of the extra oxygen in the Bi_2O_2 layers.

Yanagisawa and co-workers attempted to use the extra oxygen model to explain the reduction in the modulation

periodicity caused by the Fe and Co substitutions for Cu.¹³ They thought that partial substitution of Cu^+ or Cu^{2+} with Fe^{3+} or Co^{3+} brings extra oxygen atoms in order to keep electric neutrality and that the extra oxygen atoms are also accepted by the Bi_2O_2 layers, thus resulting in the decrease in the modulation periodicity. However, the analysis of Raman spectra of the Fe- and Co-doped samples as shown in Fig. 3 does not seem to support their explanation. If the extra oxygen atoms introduced by Fe or Co replacement for Cu are surely incorporated to the Bi_2O_2 layers, the vibration feature of the extra oxygen atoms in the Bi_2O_2 layers is supposed to

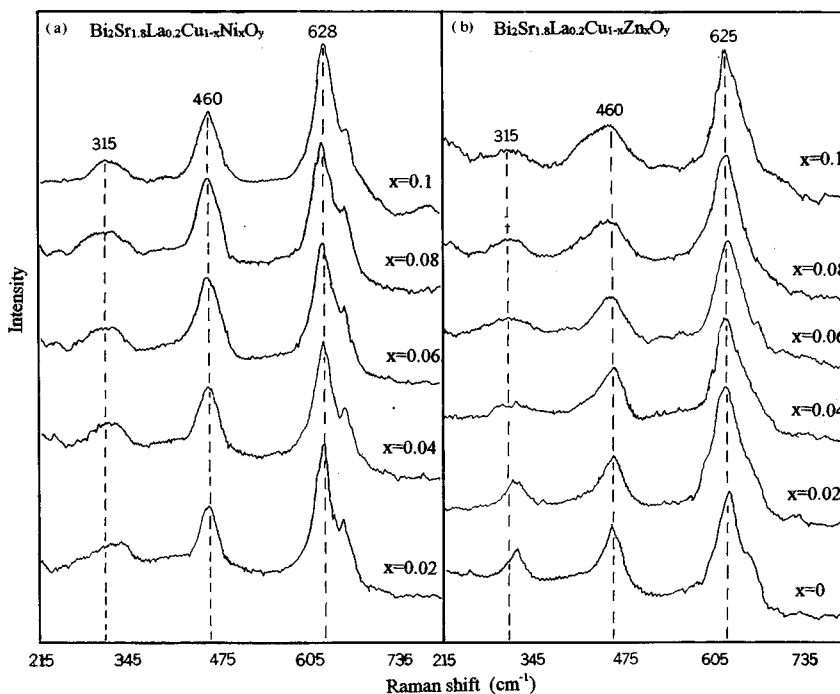


FIG. 4. Raman spectra in $\text{Bi}_2\text{Sr}_{1.8}\text{La}_{0.2}\text{Cu}_{1-x}\text{M}_x\text{O}_y$ ($M=\text{Ni}$ and Zn).

exhibit an obvious change with Fe or Co substitution. It can be expected that the vibration mode of the extra oxygen atoms should enhance in intensity with increasing dopant concentration. But, in contrast, the most prominent feature observed in the Raman spectra in Fig. 3 is that the relative intensity of the vibration mode of the oxygen atoms in the Bi_2O_2 layers (including the extra oxygen atoms corresponding to the 645-cm^{-1} mode and the oxygen atoms corresponding to the 615-cm^{-1} mode) decreases remarkably with Fe or Co doping, while the linewidth of this mode increases accordingly. This implies that there is no extra oxygen intercalated into the Bi_2O_2 layers with the Fe or Co substitution for Cu. Hence the decrease in the modulation periodicity caused by the Fe or Co doping cannot be explained by the extra oxygen model. On the other hand, one knows that the Ni or Zn substitution for Cu does not change the oxygen content of the $\text{Bi}_2\text{Sr}_{1.8}\text{La}_{0.2}\text{Cu}_{1-x}\text{M}_x\text{O}_y$ system. The extra oxygen model also cannot give a more rational interpretation for the reduction in the modulation periodicity caused by the Ni or Zn doping, as well as for the difference in the change in the modulation periodicity between the Fe- and Co-doped systems as shown in Fig. 2.

The above analysis shows that the extra oxygen model is deficient in interpreting the changes in both modulation and vibration properties of the O_{Bi} atoms caused by the Fe or Co doping. We have already pointed out that the misfit model is much more effective in interpreting the modulation change induced by doping with different elements. Therefore, we apply the crystal misfit model to examine the change in the modulation caused by Fe, Co, Ni, and Zn dopings. The crystal misfit model indicates that the superstructural modulation of Bi cuprates comes from the crystal misfit along the b axis between the Bi_2O_2 layers and the perovskite blocks. The degree of crystal misfit mainly depends on the size of the perovskite block (primarily the length of the b axis); the larger the b parameter, the lower the degree of crystal fit.^{9,11} XRD analysis has shown that in the $\text{Bi}_2\text{Sr}_{1.8}\text{La}_{0.2}\text{Cu}_{1-x}\text{M}_x\text{O}_y$ ($M = \text{Fe, Co, Ni, and Zn}$) series, Fe, Co, Ni, and Zn substitutions for Cu increase the length of the b axis. This means that the degree of the crystal misfit between the rocksalt units of the Bi_2O_2 layers and perovskite blocks enhances with the occupation of Fe, Co, Ni, or Zn in the Cu sites. The distorted Bi_2O_2 layers are certain to be rearranged in the situation of the enhancement in the degree of crystal misfit, thus resulting in the decrease in the modulation periodicity. This point agrees well with the experiment result. Nevertheless, it is worthwhile to note that though the Fe and Co dopings have a similar effect on the lattice parameter b , the Fe doping decreases the modulation periodicity more markedly than the Co doping. This suggests that lattice parameter b is not the only structure factor determining the degree of crystal misfit.

B. Dependence of the vibration properties of the oxygen atoms in the SrO and Bi_2O_2 layers on the modulation characteristic

Raman scattering analysis has shown that the vibration properties of both O_{Sr} and O_{Bi} atoms vary with the characteristic of the superstructural modulation. In the Fe- and Co-doped systems, it can be seen clearly that the vibration mode of the O_{Bi} atoms not only broadens with a decrease in intensity, but also shifts to the lower-frequency side with a de-

crease in the modulation periodicity. At the same time the vibration mode of the O_{Sr} atoms also exhibits broadening with a decrease in intensity. Such a varying behavior of the vibration modes of the O_{Sr} and O_{Bi} atoms can also be interpreted in terms of the crystal misfit model.

Onoda and Sato¹⁹ point out that the modulation wave in the Bi-2201 phase causes expansion of each layer, i.e., displacements of Bi, Sr, and Cu in the chains which run along the c axis. Since the substitutions of Fe, Co, Ni, and Zn for Cu enhance the degree of the crystal misfit between the Bi_2O_2 layers and perovskite blocks, in accordance with the argument of Onoda and Sato, it can be believed that the structure relaxation caused by the enhancement of the degree of crystal misfit is certain to enhance the relative displacements of Bi, Sr, and Cu, thus intensifying the local structure distortion. Therefore, it can be expected that the linewidth of the Raman peaks of the O_{Bi} and O_{Sr} atoms increases gradually with Fe, Co, Ni, and Zn substitutions for Cu and the intensity of the Raman peaks decreases correspondingly. This point is consistent with the experimental result obtained in the Fe- and Co-doped systems. Nevertheless, in the Ni- and Zn-doped systems the change in the 615-cm^{-1} Raman mode is not obvious due to the poorer solubility of Ni and Zn. On the other hand, the decrease in the vibration frequency of the O_{Bi} atoms observed in the Fe- and Co-doped systems is also likely to be related to the structural relaxation of the layers.

Based on the above analysis, we can say that the degree of the crystal disorder in the SrO and Bi_2O_2 layers, i.e., local structure distortion, enhances with the decrease in the modulation periodicity. Since the Fe doping decreases the modulation periodicity more strikingly than the Co doping at the same dopant concentration, it can be deduced that the degree of the local structure distortion caused by the Fe doping should be higher than that caused by the Co doping. The evidence for this postulation can be found from the Raman spectra shown in Figs. 3(b) and 3(c). That is, the Fe doping makes the vibration modes of the O_{Sr} and O_{Bi} atoms broaden more eminently than the Co doping at the same dopant concentration. The difference in the vibration property of the O_{Sr} atoms between the Ni- and Zn-doped systems also provides confirmation for this explanation.

V. CONCLUSION

We have studied the modulation structure of the $\text{Bi}_2\text{Sr}_{1.8}\text{La}_{0.2}\text{Cu}_{1-x}\text{M}_x\text{O}_y$ ($M = \text{Fe, Co, Ni, and Zn}$) series, as well as the structure distortion associated with the change in the incommensurate modulation by means of XRD, ED, and Raman scattering. Our experimental data reveal that all the substitutions of Fe, Co, Ni, and Zn for Cu decrease the modulation periodicity. The Fe substitution decreases the modulation periodicity more remarkably than the Co, Ni, and Zn substitutions at the same dopant concentration. The phonon vibration properties of the O_{Sr} and O_{Bi} atoms depend on the characteristic of the incommensurate modulation. The two Raman modes not only reduce in intensity, but also broaden gradually with a decrease in the modulation periodicity. At the same time, the O_{Bi} Raman peak also shifts to the lower-frequency side. This suggests that the local structure

distortion in the SrO and Bi_2O_2 layers intensifies with a decrease in the modulation periodicity. All these experiment results cannot find an explanation from the extra oxygen model, but can be best understood by the crystal misfit. As a result, we strongly support the argument that the origin of the

superstructural modulation in Bi cuprates comes from the crystal misfit between the Bi_2O_2 layers and perovskite blocks and that the intercalation of the extra oxygen in the Bi_2O_2 layers can only be considered a consequence caused by the crystal misfit.

-
- ¹J. M. Tarascon, Y. Lepage, P. Barboux, B. G. Bayley, L. H. Green, W. R. Mckinnon, G. W. Hull, M. Giroud, and D. M. Hwang, *Phys. Rev. B* **37**, 9382 (1988).
- ²H. W. Zandbergen, W. A. Groen, F. C. Mijhoff, G. Tendeloo, and S. Amelinckx, *Physica C* **156**, 325 (1988).
- ³O. Eibel, *Physica C* **168**, 215 (1990).
- ⁴P. L. Gai, M. A. Subramanian, and A. W. Sleight (unpublished).
- ⁵X. B. Kan and S. C. Moss, *Acta Crystallogr. B* **48**, 122 (1992).
- ⁶P. L. Gay and P. Day, *Physica C* **152**, 335 (1988).
- ⁷A. K. Cheetham, A. M. Chippendale, and S. J. Hibble, *Nature* **333**, 21 (1988).
- ⁸H. Niu, N. Fukushima, S. Takeno, S. Nakamura, and K. Ando, *Jpn. J. Appl. Phys.* **28**, L784 (1989).
- ⁹Mao Zhiqiang, Fan Chenggao, Shi lei, Yao Zhen, Yang Li, Wang Yu, and Zhang Yuheng, *Phys. Rev. B* **47**, 14 467 (1993).
- ¹⁰A. Q. Pham, M. Hervieu, A. Maigman, C. Michel, J. Provost, and B. Raveau, *Physica C* **194**, 243 (1992).
- ¹¹Mao Zhiqiang, Tian Mingliang, Tan Shun, Zuo Jian, Xu Yang, Wang Yu, Xu Chunyi, and Zhang Yuheng, *Phys. Rev. B* **49**, 6265 (1994).
- ¹²S. Amelinckx and G. Van Tendeloo, *Physica C* **235–240**, 162 (1994).
- ¹³K. Yanagisawa, Y. Matsui, T. Hasegawa, and T. Koizumi, *Physica C* **208**, 51 (1993).
- ¹⁴J. M. Tarascon, P. F. Miceli, P. Barboux, D. M. Hwang, G. W. Hull, M. Giroud, and L. H. Greene, *Phys. Rev. B* **39**, 11 587 (1989).
- ¹⁵M. Cardona, C. Thomsen, R. Liu, H. G. Vonschnering, M. Hartweg, Y. F. Yan, and Z. X. Zhao, *Solid State Commun.* **66**, 1225 (1988).
- ¹⁶R. Liu, M. V. Klein, P. D. Han, and D. A. Payno, *Phys. Rev. B* **45**, 7392 (1992).
- ¹⁷S. Sugai and M. Sato, *Jpn. J. Appl. Phys.* **28**, 1361 (1989).
- ¹⁸Mao Zhiqiang, Zhang Hongguang, Tian Mingliang, Tan Sun, Xu Yang, Wang Yu, Zuo Jian, Xu Cunyi, and Zhang Yuheng, *Phys. Rev. B* **48**, 16 135 (1993).
- ¹⁹M. Onoda and M. Sato, *Solid State Commun.* **67**, 799 (1989).